Investigation on Shear Capacity of Reinforced Concrete T-Beams Using 3D Nonlinear Finite Element Analysis

Withit PANSUK*, Yasuhiko SATO**, Tamon UEDA***, Ryosuke TAKAHASHI****

*Graduate Student, Graduate School of Eng., Hokkaido University, Kita-ku, Sapporo, 060-8628
**Dr. of Eng., Research Associate, Graduate School of Eng., Hokkaido University, Kita-ku, Sapporo, 060-8628
***Dr. of Eng., Associate Professor, Graduate School of Eng., Hokkaido University, Kita-ku, Sapporo, 060-8628
****Dr. of Eng., Research Engineer, Geotechnical and Structural Engineering Department,
Port and Airport Research Institute, Nagase, Yokosuka, 239-0826

In this paper, how the flange width affects shear capacity of RC T-beam with and without shear reinforcement is discussed based on data analysis using previous experimental results. Furthermore, 3D nonlinear finite element analyses are carried out to clarify the influence of flange width to shear resisting mechanism and shear strength. This paper presents that the finite element analysis can simulate experimental results well and shear stress distribution along flange width of T-beams is very important influential factor governing the increasing strength due to the top flange area of beams.

Key Words: T-beams, Flange Width, Shear Strength, 3-D Finite Element Method

1. Introduction

Mechanism of shear failure in plain concrete as well as reinforced concrete has been a long-standing key problem, which is not fully clarified and argued from various angles.

Recently, study on shear resisting mechanism by finite element method has received considerable attention because of its advantages. For example, the well-confirmed finite element program can reduce the lost time and cost for real experiment. Of course the most important benefit of the method is enable to evaluate damage such as cracking and crushing of concrete visually and quantitatively.

As well known, in the current JSCE design code, shear strength can be calculated based on the modified truss theory. In the equation effect of top flange width of T-beam cannot be considered. However the area of top flange may affects shear capacity when a beam would fail in shear compression mode. To predict the shear capacity of T-beam more precisely, the effect on shear resisting mechanism must be clarified.

In this paper, how the flange width affects shear capacity of RC T-beam with and without shear reinforcement is discussed based on data analysis using previous experimental results. Furthermore, shear behavior of T-beams is simulated by 3D finite element analysis with the aim of applicability verification of the analysis and how shear stress distribution along flange width differs for different flange widths is discussed through the analytical investigation.

2. Shear Capacity of RC T-beams Observed in Previous Studies

To eliminate factors and variables that affect shear-resisting mechanism of beams, the data observed in the previous studies are collected and divided into small groups with similar beam parameters and only T-beams data with different flange width are considered. The picked up data included only simple-span beams under one or two symmetrical concentrated loads. All beams failed in shear failure mode. The relevant information pertaining to sources of data, geometry, materials, and number of beams is summarized in Table 1.

From the Fig.1, in the case of T-beams without web reinforcement, the ratio of flange width to web width has almost no effect on the ultimate shear capacity of T-beams. It can be said from Fig.2, on the other hand, that in the case of T-beams with shear reinforcement, shear strength of reinforced concrete T-beams increases as the ratio of flange width to web width becomes large. The facts in turn raise question as to the effect of increased flange width on shear resistance and lead to the study

of this variable on T-beams with shear reinforcement in the web.

Table 1 Experimental data of T-beams

Test series	a/d	$\rho_w f_w$ (MPa)	Amount of data
Moayer and Regan[1]	2.4 - 3.5	0.7 - 1.1	4
Ferguson and Thompson[2]	3.4 - 6.2	*	8
Al-Alusi[3]	3.4 - 6.5	*	8
Placas and Regan[4]	3.4 - 3.6	0.4 - 1.2	19
Withey[5]	3.0	0.5 - 1.4	8
Taub and Neville[6]	3.0	0.3 - 1.3	7

Note: All beams failed in shear failure mode

f_c' = 11-57 MPa, ρ_l = 0.01-0.05

* = No data of RC beam with shear reinforcement

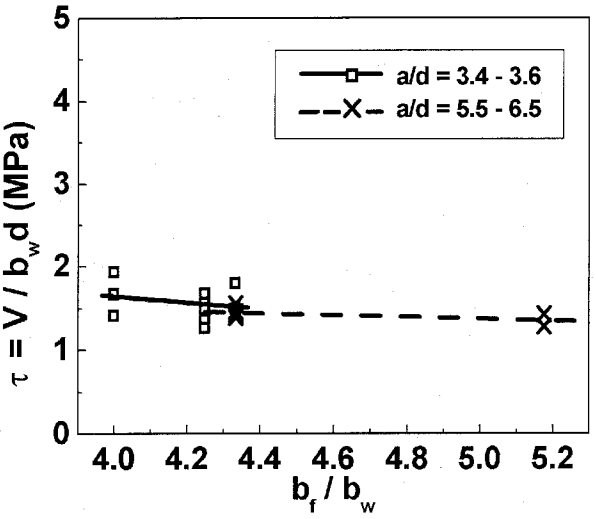

Fig.1 Shear strength of T-beams without web reinforcement

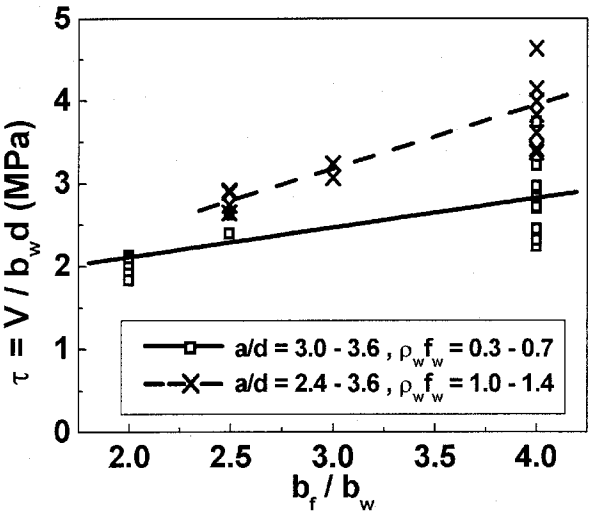

Fig.2 Shear strength of T-beams with web reinforcement

3. Outline of Finite Element Analysis

In the present study, the 3D nonlinear finite element program that has been developed at this Hybrid Structure Engineering Laboratory of Hokkaido University is used. Three-dimensional 20 nodes iso-parametric solid element, which contains 8 Gauss points, can be used for representation of plain and reinforced concrete elements.

The nonlinear iterative procedure is controlled by the modified Newton-Raphson method. In the procedure, the convergence is judged by Σ(Residual force)^2/Σ(Internal force)^2 and the limit value is set to 10^{-6} through a sensitivity analysis.

The smeared concept and the fixed crack model are adopted. When taking consideration to the case of three cracks occurs at one Gauss point, the application method for each constitutive law is to change the crack from the local coordinate system indicating the principle stress to the plane coordinate system. The constitutive laws used in the program are described below.

Stress of the reinforced concrete elements are expressed by the superposition of the behavior of steel and concrete, at this point, tri-linear model presented by Maekawa et al[7] expressing a reduction of the rate of the strain hardening in the large strain region is adopted.

The 3D Elasto-Plastic Fracture Modal[8)-10)] is adopted for the concrete before a crack. The adopted failure criteria that acted in agreement with Niwa's model in tension-compression zone and Aoyanagi and Yamada's model in tension-tension region are extended to three-dimensional criteria by satisfying boundary conditions[11].

When the first crack occurs, the concrete element under uni-axial stress in the direction perpendicular to crack plane within the local coordinate system is calculated by Reinhardt's tension- softening model[7]. Besides, in other two axes, which intersect perpendicularly which the maximum principle stress, the model proposed by Vecchio&Collins[7] is used for the principle stress-strain relationship. Shear stress acting on the plane intersecting perpendicularly with a crack, is computed by using the average shear stiffness between shear stiffness of crack plane and shear stiffness from the concrete, which does not contain any cracks. Also, a simplified model of shear transfer model developed by Li and Maekawa et al[7] is used in the present finite element program.

At the time of second and third crack, the active crack method[11] that considers the change of concrete element by focusing on the crack width is adopted. However, since this method cannot apply when 2 non-intersecting cracks occur at the same time, the concrete model for the cracks in parallel direction and averaged shear stiffness model must be applied. In terms of averaged shear stiffness model, stress calculated in the sub crack coordinate system is converted to the active crack coordinate system. And, from this shear stress and shear strain in the active crack coordinate system, the stiffness of this region

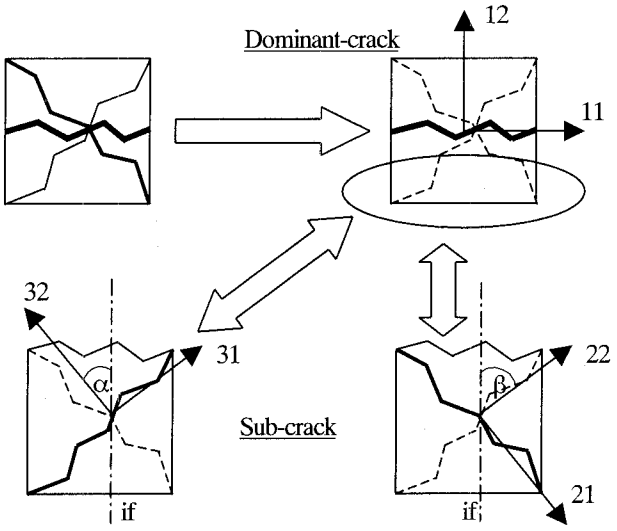

Fig.3 Criteria for consideration several sub cracks

can be obtained. The compression-tension model is the same as already stated above. Moreover, in the case of several sub cracks occur, this method is adopted to only the sub crack that have a largest strain component ($\varepsilon_{32}\cos\alpha$, $\varepsilon_{22}\cos\beta$) in the direction intersecting perpendicular to dominant crack (direction 12) after strains within the global coordinate system are converted to each sub crack coordinate system, as shown in Fig.3.

Failure criteria are judged based on load-displacement curve of the member. It can be said that the analytical member is failed after the strain-softening part takes place following the peak load. Also, type of failure can be distinguished by checking the stress-strain relationship of materials. The strain-softening characteristics that may be found will indicate an existing of failure at the location of Gauss points. When the strain-softening parts of shear stress-strain relationship are found, it means the shear failure is happened at the location of those Gauss points.

4. Validation of the 3D Nonlinear FE analysis

4.1 Experimental and analytical specimens

A general validation of the nonlinear finite element program for RC T-beams used in the present work is carried out by comparison with four beam specimens tested by Leonhardt and Walther[12] in which the shape of cross-section was chosen as an experimental parameter. The constant beam parameters for all specimens are shown in Table 2. As well as, the loading pattern and the cross section of beams are shown in Figs.4 and 5, respectively.

In the analysis, the quarter model of a beam specimen, as shown in Fig.6, is used to save calculation time and memory usage in analytical process.

4.2 Results and discussion

As shown in Table 3, the ratio of predicted ultimate load by

Table 2 Constant beam data for program validation

Beam	a/d	d	f_c' (MPa)	f_y (MPa)	f_w (MPa)
All	3.5	300	23	422	315

Table 3 Beam data for program validation

Beam	ρ_l	V_{uE} (kN)	V_{uA} (kN)	V_{uA}/V_{uE}	Mode
ET1	0.01	235	258	1.10	Flex.
ET2	0.03	235	245	1.04	Shear
ET3	0.04	235	236	1.00	Shear
ET4	0.08	176	172	0.98	Shear

observed ultimate load ranges between 0.98 and 1.10. It is important to note that all beams have different web width, and the program can predict the ultimate load very well. Also, a comparison based on these experimental evidences has indicated that T-beam with larger web width has a higher strength than similar T-beam with smaller web width.

In the beam specimen ET2, shear compression failure takes place in the concrete compression zone near loading point as shown in Fig.7. In order to compare the failure location with numerical result, the Gauss points from the many locations are selected and the shear stress-strain relationships on the plane *yz* of the global coordinate system are considered. Finally, the strain-softening portion in shear stress-strain curves which indicates fracture of concrete is found from the Gauss points in the marked area in Fig.8(a). The shear stresses from 3 selected Gauss points start to drop at the same load step as the load-displacement curve of whole beam as shown in Fig.8(b). It can be said, therefore that the concrete localized failure in the marked area caused the shear failure of the beam.

In the case of specimen ET4 with smaller web width, the same investigation method is applied. It is found that the strain-softening part in shear stress-strain curves occurs for Gauss points located in the web of the center of shear span, where is the same location as the crushing zone observed in the experiment before the ultimate load. The experimental and numerical crack pattern, and shear stress-strain curve on global coordinate system of 3 selected Gauss points are shown in Figs. 9, 10(a) and 10(b), respectively. In the analysis, finally, the beam ET4 failed by the localized failure around the loading point as well as specimen ET2.

As Figs.8(b) and 10(b) show, the symbols representing to crack in the numerical results have generally 2 types, line and rectangular shapes. The line type is the cracks that crack plane intersect perpendicularly to observation plane (plane *xy*). For cracks that crack plane intersect not perpendicularly to observation plane, the figure of cracks is shown by rectangular shape. The direction of figures is sketched from the crack angle.

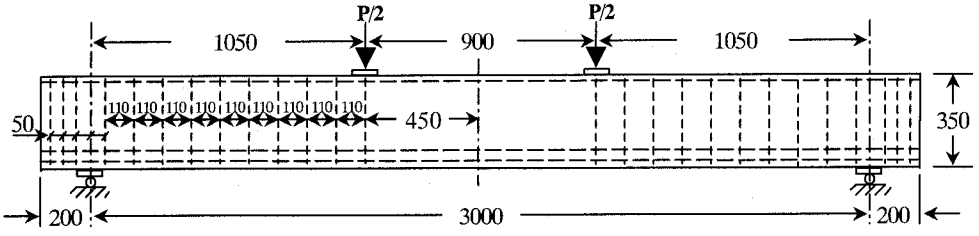

Fig.4 Loading pattern and stirrup arrangement (unit : mm)

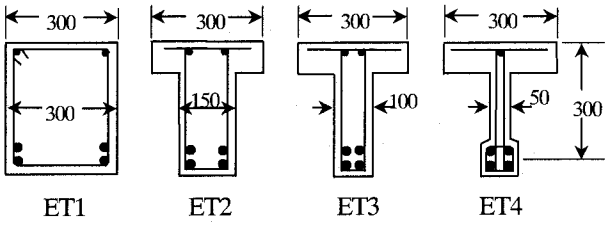

Fig.5 Beam cross sections for program validation (unit : mm)

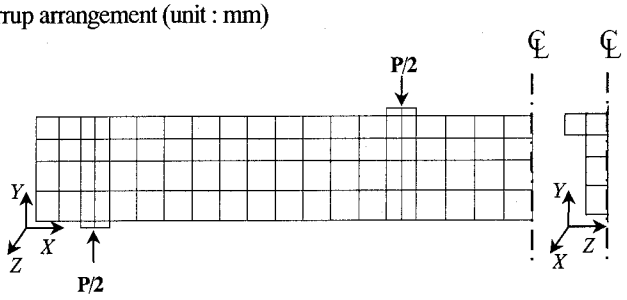

Fig.6 The quarter of specimen showing finite element mesh

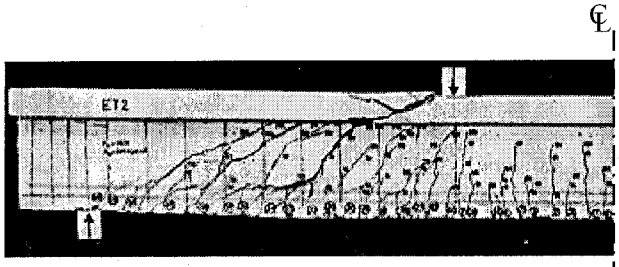

Fig.7 Crack pattern of experimental beam ET2

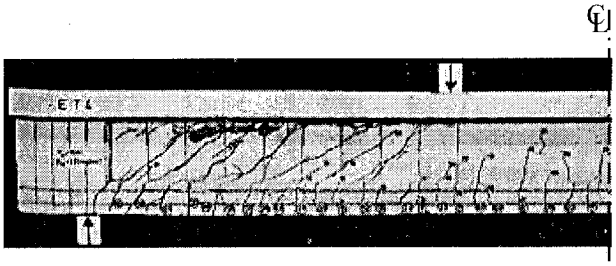

Fig.9 Crack pattern of experimental beam ET4

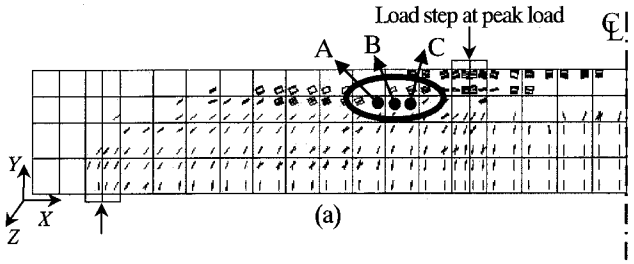

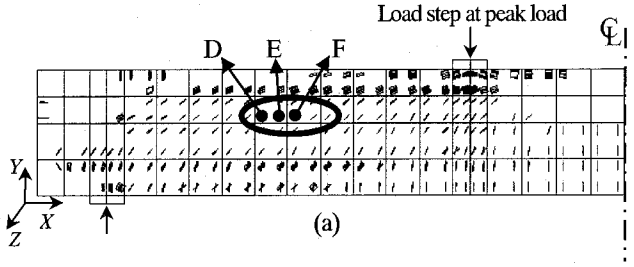

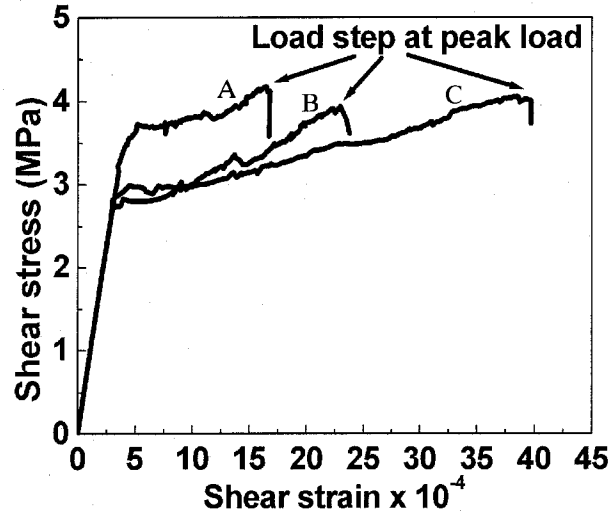

(b)

Fig.8 (a) Crack pattern of analytical beam ET2, (b) stresses-strain relationship computed from selected Gauss points A, B and C on the plane *yz* of the global coordinate system

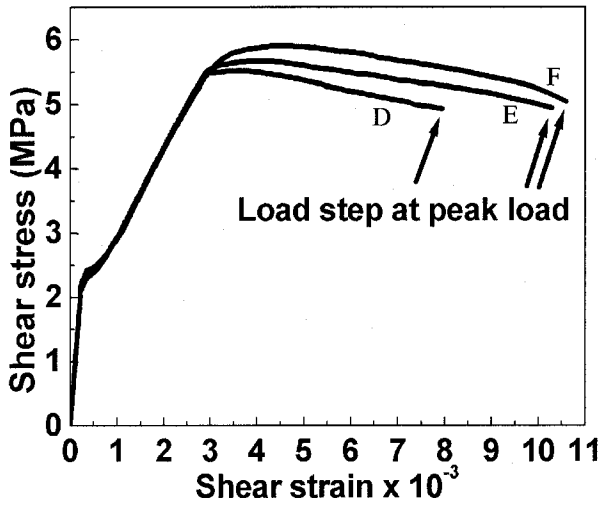

(b)

Fig.10 (a) Crack pattern of analytical beam ET4, (b) stresses-strains relationship computed from selected Gauss points D, E and F on the plane *yz* of the global coordinate system

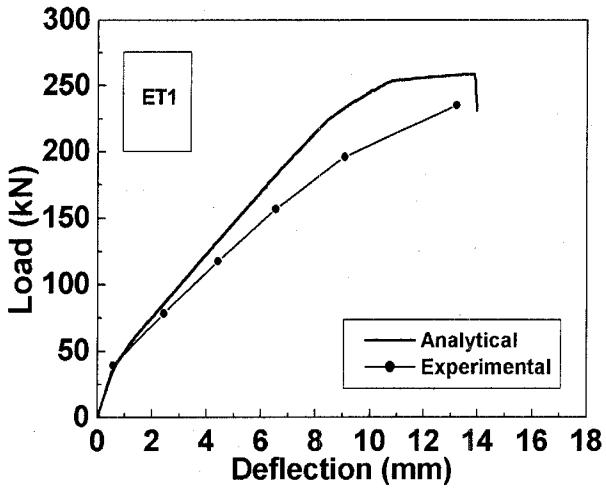

(a) b_w = 300 mm

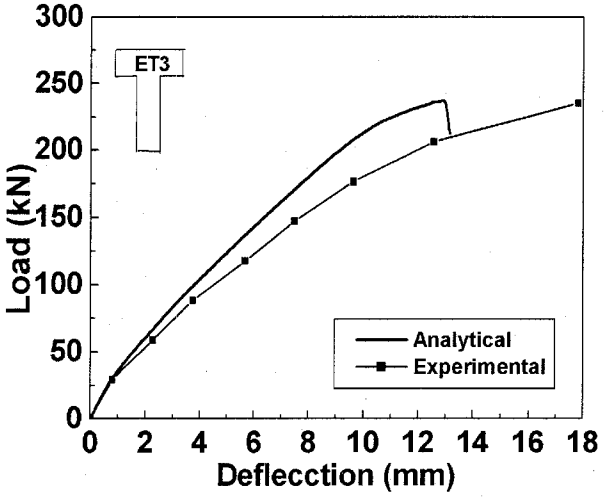

(c) b_w = 100 mm

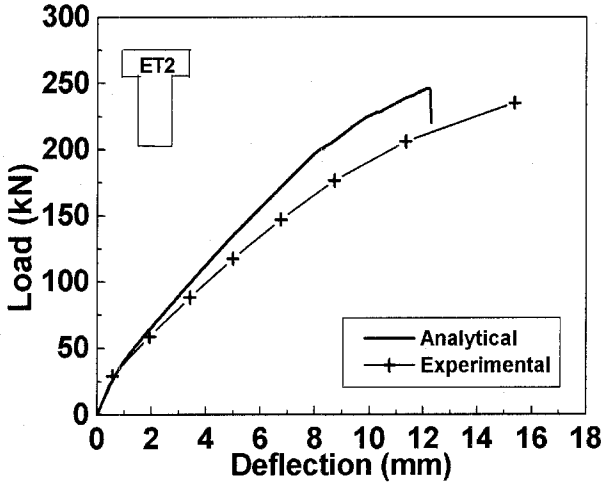

(b) b_w = 150 mm

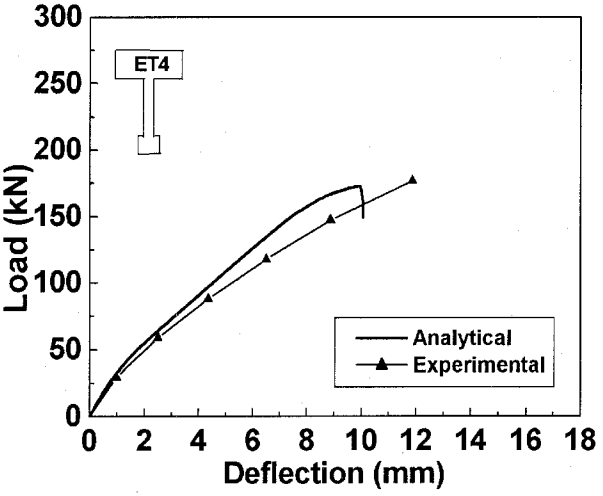

(d) b_w = 50 mm

Fig.11 Comparison of analyzed and measured load-deflection response of picked up data[12)]

The numerical and experimental load-deflection curves for each specimen are compared in Fig.11. It can be seen that the experimental and numerical ultimate load are well predicted, in both cases for those specimens failed in shear and flexure failure mode. In the view of the good correlation between analysis model and tested data, it seem that this numerical method can be used with confident for studying shear problem in reinforced concrete T-beams with similar cross sections with the data that have already been validated at this section.

5. Analytical Investigation on Effect of Flange Width

5.1 Outline of parametric study

A parametric study using the 3D FEM is carried out to clarify the effect of flange width in T-beams on shear resisting mechanism and shear capacity. The analytical specimens are subjected with 2 concentrated loads over a simple span length of 3000 mm, as the same in Fig.4. For confident investigation, these analytical specimens are based on the cross section and material properties of specimen ET2 shown in the last chapter. In the parametric study, only flange width is changed from 150 mm to 600 mm. The cross-sectional dimensions of all beam specimens are shown in Fig.12.

The mesh size and the increasing rate of prescribed displacement given at a loading point are the same for these specimens. It is also important to note that yield strength of main steel reinforcement have to increase up to about 550 MPa from the original value to prevent flexural failure. The constant material properties for all specimens are shown in Table 4.

5.2 Shear strength

Table 5 gives the information concerning the ultimate shear force and shear strength of four analytical T-beams with varying flange width, together with the ratio of flange width to web width.

Figure 13 shows predicted load-deflection curves for four analytical T-beams with varying flange width (T1, T2, T3 and T4). Because of sufficient providing main steel reinforcement, all beams are supposed to fail in shear failure mode. Load gradually increases with increasing of deflection at mid span of

beam until the drop. The drop at peak load shows that the shear failure is already occurred in the analytical beams. From the curves, beams with larger width of flange show higher ability in resisting shear force until ultimate condition more than beams with smaller flange width. At the same load level, beams with smaller width of flange have a larger deformation than beams with larger flange width. It can be said from the different in shape of curves that the flange width affects not only shear capacity but also other characteristics, such as stiffness and deformability, of T-beams.

Figure 14 demonstrates the responses of ultimate shear capacity of T-beams with varying width of flange in the increment of flange width comparing with web width. The shear strength of beam increases with a higher value of flange width comparing with web width. However, the relationship between the increment in shear capacity of T-beam and the increment of flange width cannot be represented by linear curve. Moreover, the rate of increment in shear strength gradually decreases and has a trend to be constant at high level of flange width. It means the underestimated shear capacity from design code due to an existing of a flange of T-beams will be constant at some level of increasing in flange width.

5.3 Shear stress in top flange

Figures 15, 16 and 17 show the shear stress distribution in a top flange of T-beams along a flange width direction of beams.

Table 4 Constant beam data for analytical investigation

Beam	a/d	ρ_l	ρ_w	f_c' (MPa)	f_y (MPa)
All	3.5	0.03	0.0034	23	542

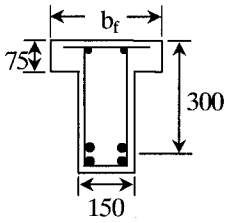

Fig.12 Cross section of T-beams for analytical investigation

Table 5 Beam data for analytical investigation

Beam	b_f (mm)	b_f/b_w	V_u (kN)	τ_u (MPa)
T1	150	1	180	4.0
T2	300	2	253	5.6
T3	450	3	292	6.5
T4	600	4	313	7.0

These figures try to express the shear resisting mechanism of reinforced concrete T-beams that causes the nonlinear relationship for shear stress increment with larger width of flange. The dotted lines in the figures represent the location of the web width and the flange width. From all three curves, the shear stress distribution along flange width is not constant at any load step. The phenomena are completely different from reinforced concrete beam with rectangular cross section. In addition, the trend of shear stress distribution is the decreasing of shear stress with the larger distance from the center of T-beams. And, the shear stress becomes zero at some distance of flange width far from the beam center. It means that the effective flange width of T-beam for shear capacity has really existed. To indicate the exactly distance of effective width of T-beam, more data are need to be investigated. In cooperation with, other factors that seem to have an effect on shear capacity of T-beams, for example, depth of top flange and reinforcement in top flange of T-beam.

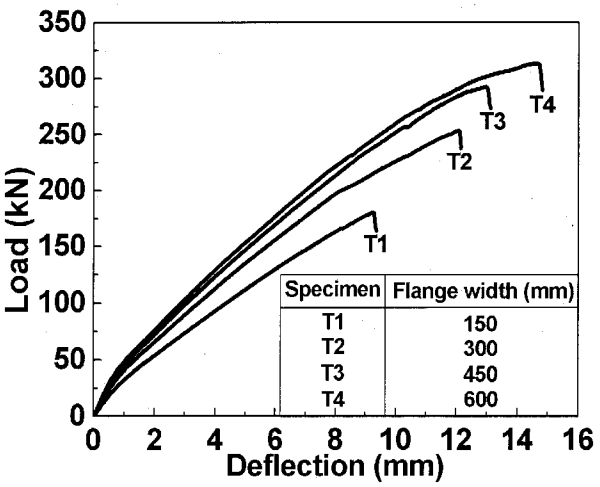

Fig.13 Comparison of analyzed load-deflection response of T-beams with varying flange width

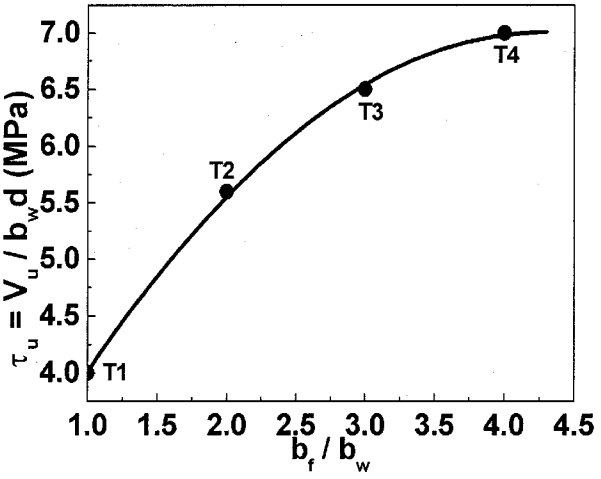

Fig.14 Shear strength of analytical T-beams with varying width of flange

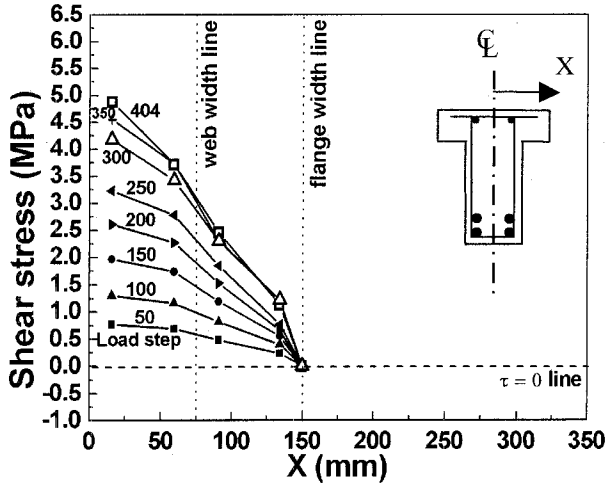

Fig.15 Shear stress distribution along flange width of T-beam T2 (b_f = 300 mm)

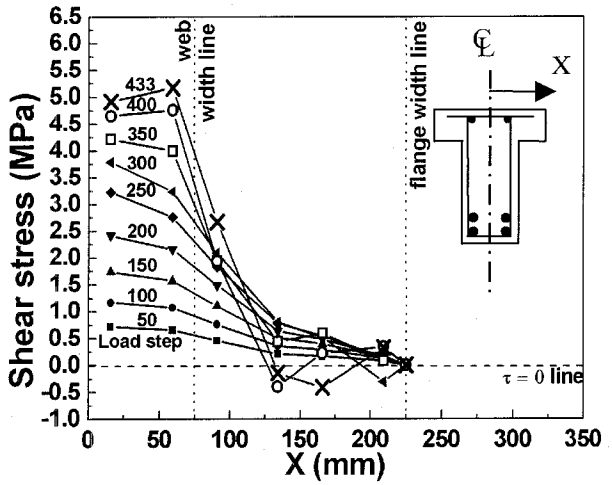

Fig.16 Shear stress distribution along flange width of T-beam T3 (b_f = 450 mm)

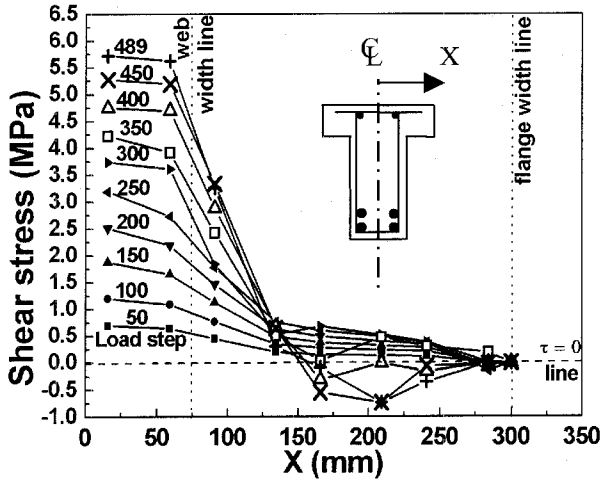

Fig.17 Shear stress distribution along flange width of T-beam T4 (b_f = 600 mm)

6.Conclusion

The following conclusions can be drawn considering the facts found in this study.

1) Increasing in flange width of T-beam gives higher shear capacity with nonlinear relationship for T-beam with web reinforcement. In the case of T-beam without web reinforcement, however, width of flange has almost no effect on shear capacity.

2) In view of the good correlation between the nonlinear finite element analysis and the experimental results, it would seem that the program can be used with confident in studying problems of shear in reinforced concrete T-beams.

3) Shear stress distribution along width of flange is not constant, decreasing and having tendency to become zero with a farther distance from beam center. As a result, the term "effective flange width" for shear capacity of T-beam has really existed and need to be clarified.

Notation

a = shear span
b_f = flange width
b_w = web width
d = effective depth
f_c' = compressive strength of concrete
f_w = yield stress of shear reinforcement
f_y = yield stress of main reinforcement
V = applied shear force
V_u = ultimate shear force
V_{uA} = ultimate shear force observed in analysis
V_{uE} = ultimate shear force observed in experiment
α, β = angle between the sub-crack plane and the dominant-crack plane
ε = strain in concrete
ρ_l = percentage of main reinforcement
ρ_w = percentage of shear reinforcement
τ = shear stress
τ_u = ultimate shear stress

Acknowledgements

This study is the part of research supported by the Japanese Government scholarship that is gratefully acknowledged. Our sincere word of thanks goes to Mr.Ryuta ABEMATSU and Mr.Yoshinori UTSUNOMIYA, graduate student; their efforts are much appreciated. Also, we would like to express our gratitude to Prof. Yoshio KAKUTA for his meaningful advice.

References

1) Moayer, M., and Regan, P. E., "Shear Strength Of Prestressed And Reinforced Concrete T-Beams," SP-42,

Shear in Reinforced Concrete, Vols. 1&2, American Concrete Institute, pp.183-213, 1974.
2) Ferguson, P. M., and Thompson, J. N., "Diagonal Tension in T-Beams Without Stirrups," ACI Journal, Mar. 1953, pp. 665-675.
3) Al-Alusi, A. F., "Diagonal Tension Strength of Reinforced Concrete T-Beams with Varying Shear Span," ACI Journal, May. 1957, pp. 1067-1077.
4) Placas, A., and Regan P. E., "Shear Failure of Reinforced Concrete Beams," ACI Journal, Oct. 1971, pp. 763-774.
5) Withey, M. O., "Tests on Plain and Reinforced Concrete: Series of 1907," *Bulletin of the University of Wisconsin* No. 197, Engineering Series, V. 4, No. 2, 1908.
6) Taub, J., and Neville, A. M., "Resistance to Shear of Reinforced Concrete Beams Part 2-Beams with Vertical Stirrups," ACI Journal, Sep. 1960, pp. 315-336.
7) Takahashi, R., Sato, Y., Ueda, T., "A simulation of shear failure of steel-concrete composite slab by 3D nonlinear FEM," Journal of Structural Engineering, JSCE, Vol.48A, Mar. 2002 (In Japanese)
8) Maekawa, K., Takemura, J., Irawan, P., and Irie, M., "Continuum Fracture in Concrete Nonlinearity Under Triaxial Confinement," Proceedings of JSCE No.460/V18, Feb. 1993, pp.113-122.
9) Maekawa, K., Takemura, J., Irawan, P., and Irie, M., "Plasticity in Concrete Nonlinearity Under Triaxial Confinement," Proceeding of JSCE No.460/V18, Feb. 1993, pp.123-130.
10) Maekawa, K., Takemura, J., Irawan, P., and Irie, M., "Triaxial Elasto-Plastic and Fracture Model for Concrete," Proceeding of JSCE No.460/V18, Feb. 1993, pp.131-138.
11) Okamura, H., Maekawa, K., "Nonlinear Analysis and Constitutive Models of Reinforced Concrete", Gihoudou 1991.
12) Leonhardt, F. and Walther, R. "Beitrage zur Behandlung der Schubprobleme im Stahlbetonbau," J. BETON-UND STAHLBETONBAU, 1962. 7. Heft 7, pp. 161-173.

(Received September 12, 2003)